



OPEN Machine learning analysis of s-EASIX for predicting 30-day mortality in sepsis patients from MIMIC-IV

Zhenghui Kong^{1,2,3}, Yuwei Liu^{1,3,4}, Huilong Chen^{1,3,5}, Hong Guo^{3,6,7}, Zhiyi Zeng⁸, Zhiyu Liu⁹ & Qiujiang Liu^{2,3}✉

Endothelial dysfunction is an important risk factor for the progression of sepsis. The simplified endothelial activation and stress index (s-EASIX) serves as an indirect measure of endothelial activation, whose dynamic changes have an unclear association with prognosis in sepsis. Therefore, we conducted this study to investigate the association between clinical subphenotypes indicated by s-EASIX trajectories and 30-d mortality in sepsis. Based on MIMIC-IV v3.1, the association of s-EASIX dynamic trajectories with 30-d mortality in sepsis was investigated in this retrospective cohort analysis. The prognostic value of trajectory patterns was verified by Kaplan–Meier curves, multivariate regression, and subgroup analyses. Machine learning models incorporating s-EASIX were established, and the weights of contribution of key variables to model decision-making were revealed using SHAP values. This study screened 8113 sepsis patients and identified five classes of s-EASIX trajectories. Cox proportional hazards regression revealed that the 30-d mortality significantly rose in Class 4 (Mid-Increasing) (HR 1.79, 95% CI 1.51–2.11) and Class 5 (High-SlowDecline) (HR 2.53, 95% CI 2.06–3.11), and it was comparable between Class 3 (High-FastDecline) and Class 1/2 (Low-Stable and Mid-Stable). The independent prognostic value of trajectory patterns was verified by multivariate regression, and the HR values for high-risk trajectories remained within 2.53–5.95 after adjusting for demographics and confounders. According to model assessment, LightGBM exhibited superior performance in the validation set (AUC 0.842, 95% CI 0.818–0.866), and its predictive reliability was proven by the Brier score (0.014 in the validation set). Moreover, we analyzed the SHAP values and identified the s-EASIX trajectory as the core variable; the model served as an interpretable tool for risk stratification and early intervention in high-risk sepsis patients. The dynamic increasing pattern of the s-EASIX trajectory correlates with the elevation of 30-d mortality in sepsis, suggesting that persistent endothelial dysfunction raises the risk of unfavorable prognosis.

Keywords Trajectory analysis, Endothelial activation and stress index, Sepsis, Endothelial dysfunction

Sepsis, a life-threatening organ dysfunction resulting from dysregulated host response to infection, has become a major cause of death globally and a common critical illness in ICU patients^{1,2}. As revealed by epidemiological data, there are approximately 48.9 million cases of sepsis annually worldwide, with 11 million deaths accounting

¹The Fifth Clinical College of Guangzhou University of Chinese Medicine, Guangzhou University of Chinese Medicine, Guangzhou 510006, Guangdong, China. ²Department of Critical Care Medicine, Guangdong Provincial Second Hospital of Traditional Chinese Medicine, No. 60, Hengfu Road, Guangzhou 510095, Guangdong, China. ³Guangdong Provincial Engineering Technology Research Institute of Traditional Chinese Medicine, Guangdong Provincial Second Hospital of Traditional Chinese Medicine, Guangzhou 510095, Guangdong, China. ⁴Department of Gastroenterology, Guangdong Provincial Second Hospital of Traditional Chinese Medicine, Guangzhou 510095, Guangdong, China. ⁵Department of Emergency Medicine, Guangdong Provincial Second Hospital of Traditional Chinese Medicine, Guangzhou 510095, Guangdong, China. ⁶Department of Geriatric, Guangdong Provincial Second Hospital of Traditional Chinese Medicine, Guangzhou 510000, Guangdong, China. ⁷State Key Laboratory of Traditional Chinese Medicine Syndrome, The Second Affiliated Hospital of Guangzhou, University of Chinese Medicine, Guangzhou 510405, Guangdong, China. ⁸Department of General Practice, The Fifth Affiliated Hospital of Sun Yat Sen University, Zhuhai 510000, Guangdong, China. ⁹School of Basic Medical Sciences, Chengdu University of Traditional Chinese Medicine, Chengdu 611137, Sichuan, China. ✉email: liuqiujiang@163.com

for nearly 20% of total global deaths³. As a result, sepsis has become a major public health threat. Rapid and appropriate management in the early stage of sepsis can effectively delay its progression, which is crucial for mitigating adverse outcomes. Nowadays, clinical research on common prognostic indicators for sepsis focuses on procalcitonin, interleukins, C-reactive protein, adrenomedullin, and lactate^{4,5}. Due to the rapid progression of sepsis and its complex pathophysiological mechanisms, physiological indicators and inflammatory status in patients undergo constant changes. Therefore, it is difficult to dynamically reflect the disease development trajectory by single-time-point measurements, thus restricting the clinical translation of available prediction models⁶. Therefore, exploring novel dynamic prognostic indicators and creating a risk stratification system holds clinical significance for improving early warning of sepsis and guiding stratified interventions.

Endothelial dysfunction is an important risk factor for sepsis progression^{7,8}. The inflammatory storm in sepsis induces endothelial activation and thus triggers endothelial inflammatory responses and up-regulation of adhesion molecules. This, as a pathological cascade, constitutes the core mechanism underlying microcirculatory dysfunction and microvascular hyperpermeability. As a result, sepsis-induced multi-organ injury ultimately deteriorates^{9,10}. Clinical research suggests that markers for endothelial dysfunction (e.g., vascular endothelial growth factor VEGF, VE-cadherin, and syndecan-1) are of critical value in predicting sepsis-induced multi-organ injury¹¹. Given their pathophysiological relevance, these markers have become important clinical indicators for monitoring sepsis and early identifying its unfavorable prognosis¹⁰.

The endothelial activation and stress index (EASIX), an indirect measure of endothelial activation, has been verified as a key prognostic factor in assessing sepsis and related systemic immune-inflammatory diseases^{12–15}. Existing studies often assess the impact of static EASIX on sepsis 30-d mortality, but it is difficult to dynamically capture the mortality in sepsis using single-time-point EASIX¹⁶. Simplified EASIX (s-EASIX), one of the common variants of EASIX, shares dynamic trends with EASIX^{16,17}. Furthermore, the creatinine value is excluded from s-EASIX calculation, which effectively avoids bias resulting from fluctuation in creatinine clearance rates in sepsis patients undergoing continuous renal replacement therapy (CRRT). Meanwhile, the dynamic trajectory of s-EASIX can reveal prognostic differences that cannot be reflected under its initial static state. This provides more discriminative evidence for assessing the progression of endothelial dysfunction and mortality risk in sepsis patients. To sum up, the s-EASIX trajectory demonstrates high superiority and accuracy in sepsis prediction.

We conducted this study to identify longitudinal trajectory patterns of s-EASIX in ICU sepsis patients based on MIMIC-IV (v3.1) and assess their association with prognosis. The findings are expected to fully elucidate the prognostic value of s-EASIX longitudinal trajectories in sepsis and inform clinical decision-making and risk stratification strategies in critical care.

Materials and methods

Data source

This retrospective cohort study was conducted based on MIMIC-IV (v3.1) in full compliance with all relevant guidelines and regulations. The Beth Israel Deaconess Medical Center (BIDMC) Institutional Review Board approved database access and granted a waiver of informed consent. All data were acquired in accordance with the relevant guidelines of MIMIC-IV¹⁸. The investigator (Zhenghui Kong) passed the Collaborative Institutional Training Initiative certification for human research ethics (Certificate No.: 63562889) and signed a data use agreement for data access. All data were rigorously anonymized in accordance with privacy standards in the *Health Insurance Portability and Accountability Act (HIPAA)*. All study procedures were carried out following the MIMIC-IV access guidelines and ethical standards.

Study population

We screened 31,911 sepsis patients, and they were diagnosed with sepsis following the Sepsis 3.0¹⁹ criteria and admitted to the ICU, with SOFA scores ≥ 2 in cases of suspected or confirmed infection. Exclusion criteria: 1) age < 18 years at the initial diagnosis; 2) ICU stay < 12 h; 3) with comorbidities (e.g., malignancy, myocardial infarction, cirrhosis) known to significantly influence LDH and platelets; 4) with missing data on LDH or platelet counts; 5) < 3 measurements of LDH or platelets within 30 days; and 6) physiologically implausible values of LDH or platelets (e.g., platelets = 0 or extreme outliers of LDH). For multiple ICU admissions, we only extracted data from the first admission. The flow chart of the study is shown in Fig. 1.

Data collection

The following five categories of baseline data were extracted: 1) Demographics: age, gender, BMI, and race; 2) Vital signs: heart rate HR, blood pressure BP, temperature, and SpO₂ at admission; 3) Laboratory indicators: white blood cells, hemoglobin, platelets, serum creatinine, lactate, LDH, albumin, international normalized ratio, prothrombin time, total bilirubin, alanine aminotransferase, and aspartate aminotransferase; 4) Scores: SOFA, LODS, and SIRS; and 5) Interventions: anticoagulants, antiplatelet drugs, vasoactive agents, tranquilizers, and CRRT or invasive mechanical ventilation. The laboratory indicators measured within 72 h after ICU admission were analyzed. Data with $< 20\%$ missing values underwent multiple imputation using the R *missForest* package. The primary outcome was the 30-d in-hospital survival rate, and the follow-up started from ICU admission until death or discharge.

Calculation of s-EASIX

The EASIX is considered an indirect measure of endothelial activation²⁰. Integrating platelets and LDH, the s-EASIX has been verified to exhibit similar trends to the EASIX^{16,17}. Based on previous studies, log transformation was performed to reduce discrete variables prior to analysis²¹. The specific formula for s-EASIX is as follows:

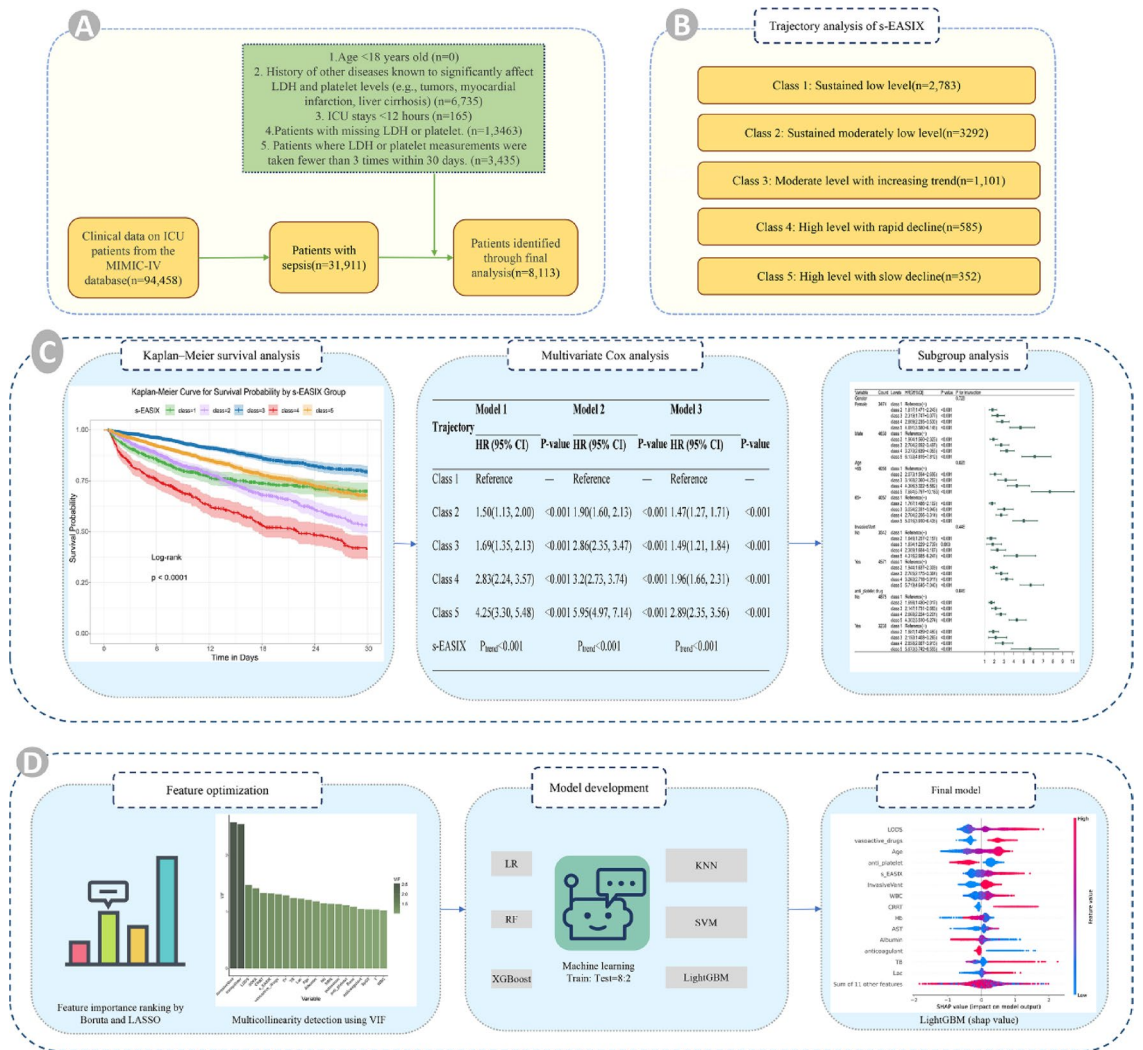


Fig. 1. Study flowchart.

$$s - EASIX = \log_2 \left(\text{LDH [IU/L]} / \text{platelet count} \left[10^9 / \text{L} \right] \right)$$

Statistical analysis

Identification of s-EASIX dynamic trajectories

The s-EASIX longitudinal trajectories were modeled using the R *flexmix* package. Specifically, the s-EASIX values were extracted from each patient within a 30-d window, and those with < 3 measurements or an interval > 30 days between the first and last measurements were excluded. Then patient subgroups with similar s-EASIX dynamic trajectories were identified by growth mixture models (GMMs) and clustered into corresponding classes. By fitting GMMs with varying numbers of latent intents (K), the optimal clustering number was determined by the -2 log-likelihood, Akaike information criterion AIC, and Bayesian information criterion BIC.

Clinical baseline data

Baseline data of skewed or normal distributions were compared by the Mann–Whitney U test or t-test, respectively. Continuous variables were presented as mean (standard deviation) or median (interquartile range IQR), and compared by the Pearson’s chi-square test. Results were described by frequency and percentage (%).

Clinical outcomes

First, the survival rate was analyzed across subgroups by Kaplan–Meier (K–M) curves. Second, the association of s-EASIX trajectory classes with the study endpoint was assessed by Cox proportional hazards regression, with HR and 95% CI calculated. The proportional hazards assumption was assessed using the Cox proportional hazards model based on the Schoenfeld residuals. Finally, stratified and interaction analyses were conducted to explore the influence of gender, age, mechanical ventilation, and antiplatelet drugs on this association, with likelihood-ratio tests done for significance in interaction.

Machine learning (ML) modeling and visualization

Data were assigned to training (80%) and validation (20%) sets. Predictor variables were first screened by the Boruta algorithm and LASSO regression. They were then tested for multicollinearity by the variance inflation factor (VIF), and those with $VIF > 5$ were excluded. Then six ML models were created and compared: logistic regression (LR), K-nearest neighbors (KNN), random forest (RF), support vector machine (SVM), XGBoost, and LightGBM. Model performance and robustness were evaluated in the validation set, with the AUC as the core metric, and overfitting was assessed by the Brier score. The model with optimal performance and robustness was selected and visually interpreted by the SHAP value to reveal the contribution of each feature to model prediction.

Results

s-EASIX trajectories and patient characteristics

With rigorous eligibility criteria, 8113 patients were ultimately included. Based on the AIC and BIC (Table S1), five classes of s-EASIX longitudinal trajectory patterns were identified (Fig. 2): Class 1: Low-Stable; Class 2: Mid-Stable; Class 3: High-FastDecline; Class 4: Mid-Increasing; Class 5: High-SlowDecline. To validate the effectiveness and robustness of the five classes of trajectory models, posterior validation (Table S2, Table S3) and trajectory pattern analysis (Table S4) were systematically conducted. The results revealed robust certainty of the model's discrimination performance, with an average posterior probability of 79.2% (median 82.0%) for all subjects. The slope parameters significantly differed across classes ($P < 0.05$), confirming the model's ability to distinguish clinical subgroups with different trajectory trends. Additionally, sensitivity analyses (Table S5, Figure S1) further revealed that even within shorter observation windows (to reduce immortal time bias), the s-EASIX dynamic trajectory could consistently identify specific subgroups while keeping its consistent associations with prognosis. This confirmed the robustness of the main findings. Baseline demographic and clinical characteristics differed significantly across these classes (Table S6 and Table S7). Based on the normality analysis of baseline characteristics, continuous and categorical variables were expressed as median (IQR) and frequency (%), respectively. Class 5 (High-SlowDecline) had the highest baseline s-EASIX value and 30-d mortality. Notably, although Class 3 (High-FastDecline) had a higher baseline s-EASIX value than Class 4 (Mid-Increasing) at ICU

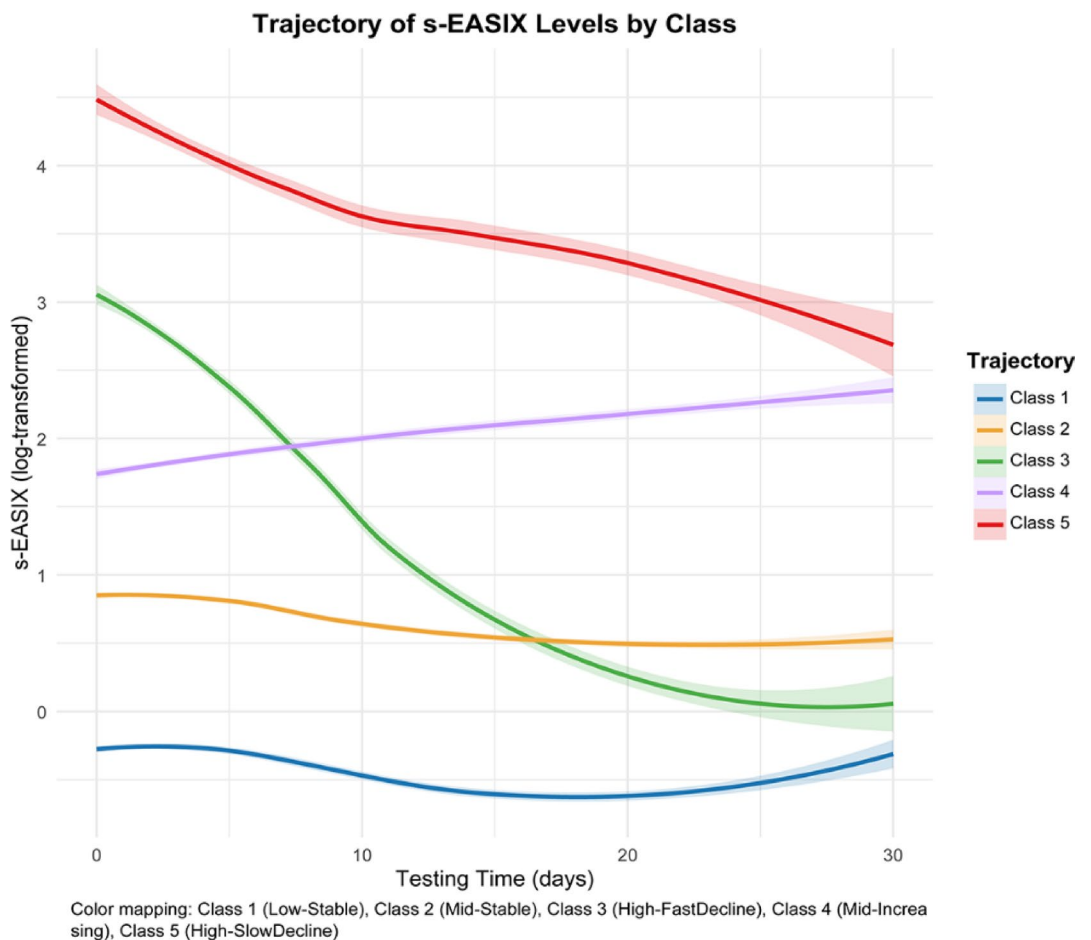


Fig. 2. s-EASIX trajectories of sepsis patients. Class 1: Low-Stable; Class 2: Mid-Stable; Class 3: High-FastDecline; Class 4: Mid-Increasing; Class 5: High-SlowDecline.

admission, and more severe conditions were revealed by initial laboratory indicators, the 30-d mortality was finally lower in the former.

s-EASIX trajectories and clinical outcomes

As revealed by K-M curves (Fig. 3), great differences were presented in survival rates among the five classes. Class 4 (Mid-Increasing) and Class 5 (High-SlowDecline) were associated with obvious elevation of mortality odds, while the 30-d mortality was comparable between Class 3 (High-FastDecline) and Class 1/2 (Low-Stable and Mid-Stable). The results of Cox proportional hazards regression aligned with the K-M analysis (Table 1). With Class 1 (Low-Stable) as the reference, the mortality odds showed significant differences across classes after multivariate adjustment. In Model 1 (crude) and Model 2 (adjusted for demographics), the 30-d mortality odds obviously elevated in Class 4 (Mid-Increasing) (Model 1: HR 3.00, 95% CI 2.57–3.51; Model 2: HR 3.20, 95% CI 2.73–3.74) and Class 5 (High-SlowDecline) (Model 1: HR 5.23, 95% CI 4.37–6.27; Model 2: HR 5.95, 95% CI 4.97–7.14). The observed association remained significant in Model 3 (fully adjusted) (Class 5: HR 2.53, 95% CI 2.06–3.11; Class 4: HR 1.79, 95% CI 1.51–2.11).

Some variables in the model violated the proportional hazards assumption. To address this issue, a time-varying Cox model was used for correction. Based on clinical course characteristics and K-M curve patterns, follow-up time was divided into three clinically meaningful phases: 0–7 d, 8–14 d, and 15–30 d. By introducing interaction terms between variables violating the proportional hazards assumption and the time-varying variables, independent estimation of hazard ratios at each time point was enabled. The analysis results showed that the effect direction, magnitude, and statistical significance of core variables in the time-varying Cox model were highly consistent with those in the original model (Table S8, Table S9).

To control for the potential influence of baseline s-EASIX, it was incorporated into the original Cox model of trajectory (Table S10). The results still confirmed the significant and independent association between each class and 30-d mortality. Additionally, an interaction analysis was conducted between each class and baseline s-EASIX (Table S11) to clarify their combined influence on mortality risk. The results revealed that higher baseline s-EASIX levels further increased mortality risk in both Class 3 and Class 5.



Fig. 3. Kaplan–Meier curves for 30-d mortality. Horizontal axis: time, vertical axis: mortality.

Trajectory	Model 1		Model 2		Model 3	
	HR (95% CI)	P-value	HR (95% CI)	P-value	HR (95% CI)	P-value
Class 1	Reference	–	Reference	–	Reference	–
Class 2	1.50(1.13, 2.00)	<0.001	1.90(1.60, 2.13)	<0.001	1.47(1.27, 1.71)	<0.001
Class 3	1.69(1.35, 2.13)	<0.001	2.86(2.35, 3.47)	<0.001	1.49(1.21, 1.84)	<0.001
Class 4	2.83(2.24, 3.57)	<0.001	3.2(2.73, 3.74)	<0.001	1.96(1.66, 2.31)	<0.001
Class 5	4.25(3.30, 5.48)	<0.001	5.95(4.97, 7.14)	<0.001	2.89(2.35, 3.56)	<0.001
s-EASIX	P _{trend} < 0.001		P _{trend} < 0.001		P _{trend} < 0.001	

Table 1. Cox analysis of associations of different trajectories with in-hospital mortality. *P*-values have been Bonferroni-corrected. HR, Hazard ratio; CI, Confidence interval. Model 1: Crude. Model 2: Adjusted for age, gender, race, temperature, SpO₂, HR, SBP, and DBP. Model 3: Adjusted for HR, SBP, DBP, SpO₂, temperature, gender, age, race, albumin, ALT, AST, Cr, Hb, INR, Lac, potassium, PT, TB, WBC, LODS, SOFA, SIRS, InvasiveVent, CRRT, vasoactive agents, anticoagulants, tranquilizer, and antiplatelet drugs; included as time-varying covariates; InvasiveVent, CRRT, and vasoactive agents.

The s-EASIX was identified by the stratified analysis as a potent predictor for prognosis across subgroups (Fig. 4). The observed association remained significant in subgroups stratified by gender, mechanical ventilation status, and antiplatelet drugs ($P_{\text{interaction}} > 0.05$), suggesting the universal predictive value of s-EASIX in mortality. To sum up, the 30-d mortality odds were the highest in Class 5 (High-SlowDecline) across all subgroups, and elevated HRs were also observed in the remaining classes ($P < 0.05$).

Specifically, age was the only variable with significant interactions ($P = 0.028$): The 30-d mortality odds in Class 4 (Mid-Increasing) and Class 5 (High-SlowDecline) were higher in younger patients (HR 4.306 and 7.684) than in older patients (≥ 65 years; HR 2.704 and 5.016).

ML modeling and visualization

Feature variables were selected by the Boruta algorithm and LASSO regression (Fig. 5). First, the Boruta algorithm screened 29 variables by assessing their “importance” (Fig. 5A), of which 25 were retained based on the minimum lambda value ($\lambda = 0.000759$) (Fig. 5B and C). The characteristics of these variables are detailed in Table S12. Subsequently, the intersection of Boruta and LASSO regression results was taken, yielding 25 variables (Fig. 5D). None of the variables had $VIF > 5$, confirming no significant multicollinearity. Finally, these 25 variables were incorporated into ML analyses.

The performance of ML models in predicting 30-d mortality odds was assessed (Fig. 6), and the specific model parameters are listed in Table S13. LightGBM demonstrated optimal generalization capability (Fig. 6A), with an AUC for its discrimination power of 0.916 (95% CI 0.907–0.924) in the training set and 0.842 (95% CI 0.818–0.866) in the validation set. Calibration curves for both sets closely approximated the ideal diagonal line (Brier score: 0.025 in the training set, 0.014 in the validation set), confirming the clinical reliability of probability predictions. Therefore, we selected LightGBM as the core model, and its clinical utility was further multidimensionally verified (Fig. 7). tenfold cross-validation of LightGBM yielded a mean AUC of 0.837 (Fig. 7A). LightGBM exhibited positive net benefits within threshold probabilities of 0–90% (Fig. 7C). The confusion matrix further revealed a sensitivity of 70% and specificity of 82% for the model (Fig. 7D). Additionally, to quantify the incremental value of the ML model, its discriminative performance (AUC) was compared with the LR model incorporating trajectories, and the significance of the difference was assessed using the DeLong test (Table S14).

To visualize the influence of LightGBM model features on the prediction of 30-d all-cause mortality, the SHAP value was calculated for each feature. Based on the mean absolute SHAP values (Fig. 8A), the s-EASIX was identified as the core variable in the model. The feature-model association is shown in Fig. 8B; red indicates high feature values (positive SHAP values), elevating the 30-d mortality odds, while blue indicates low feature values (negative SHAP values). It can be seen that increases in feature values of LODS, age, and s-EASIX positively elevated the model output (elevated 30-d mortality odds). Meanwhile, the clinical effect patterns of key features were elucidated by SHAP dependence analyses (Fig. 8D).

Furthermore, to visually present model interpretability, we analyzed one case of a 67-year-old man who died during hospitalization. LODS (+0.92) and s-EASIX (+0.86) greatly influenced 30-d mortality in this death case (Fig. 8C). Other contributors included lactate (+0.70), followed by vasoactive agents (−0.34) and antiplatelet drugs (+0.30). These results verified the model’s clinical decision-making logic.

Discussion

To our knowledge, this study identified heterogeneous trajectories of s-EASIX in sepsis patients for the first time and investigated the association of s-EASIX changes with 30-d mortality. Moreover, a prediction model was created for the survival probability in sepsis patients based on s-EASIX. Our findings suggest that the prediction model can capture biomarker changes and achieve more accurate prognostic prediction as compared to single-time-point EASIX.

The obvious association of LDH and platelets with adverse outcomes in sepsis has been verified by numerous clinical studies, and the two are identified as important indicators for poor prognosis^{22–24}. Research suggests that high LDH is closely linked to elevated mortality²², and a rapid decline in platelet counts serves as a key prognostic

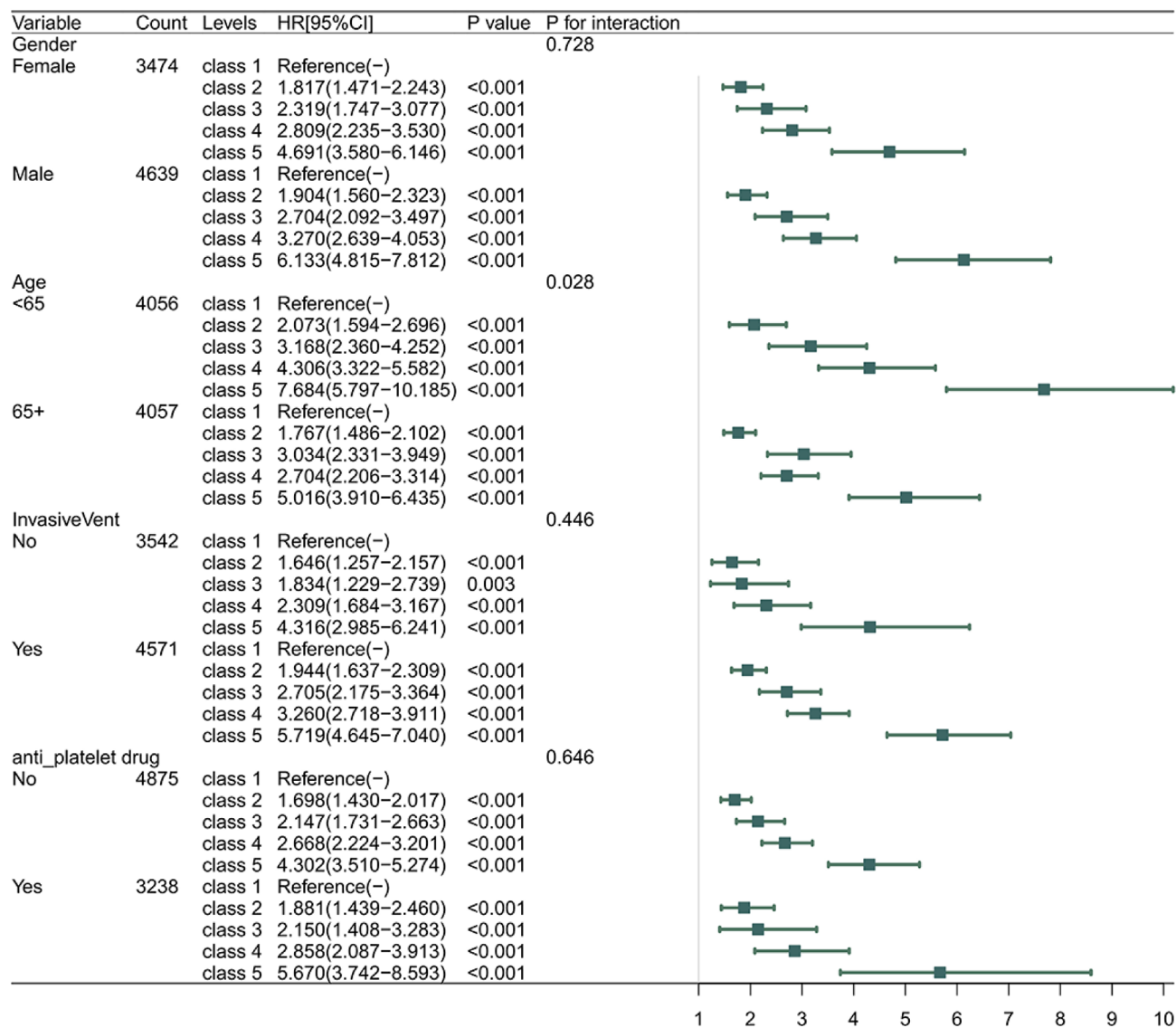


Fig. 4. Forest plot for subgroup analyses.

factor predicting sepsis mortality²⁵. In sepsis patients, however, the accuracy of assessing the trend of lactate and platelet counts alone is insufficient. Elevation of LDH, as a non-specific marker of cell injury, may stem from multiple pathophysiological processes (e.g., tissue hypoxia, inflammatory response, hemolysis, or hepatic/renal dysfunction)²⁶. As a result, it is difficult to accurately reflect the pathological mechanism of endothelial injury in sepsis. Moreover, LDH levels are susceptible to underlying diseases, restricting the clinical interpretation of a single measurement value. Besides, platelet counts can fully reflect coagulation, inflammation, and endothelial status. However, a decline in platelet counts in sepsis patients may result from infection, drugs, and immune factors, with rapid fluctuations following treatments such as anti-infective therapy, fluid resuscitation, vasoactive agents, and organ support. As a result, platelet counts lack sensitivity and accuracy in predicting disease progression, restricting their clinical use²⁷. Consequently, it is difficult to capture changes in disease progression by single-time-point measurements of platelets. Moreover, the association of platelet changes with prognosis is often obscured by static assessment of a single indicator, particularly following infection control or intervention. In contrast, s-EASIX can compensate for the shortcomings of any single indicator in specificity, robustness, and dynamic sensitivity. Moreover, it more accurately reflects the persistence of endothelial injury, the progression of microcirculatory dysfunction, and the body's responsiveness of sepsis patients to treatment. With dynamic trajectories of the s-EASIX, the synergistic changes in LDH and platelets can be captured during disease progression, providing a more comprehensive and timely clinical reference for prognostic evaluation in sepsis²⁸.

Endothelial cells, central to the pathophysiology of sepsis, are crucial players in regulating microcirculation and maintaining the integrity of organ and tissue barriers. In sepsis, immune cells are activated to massively release inflammatory mediators, directly damaging vascular endothelial cells. As a result, the barrier function of vascular endothelial cells is compromised and vascular permeability increases, resulting in dysregulation

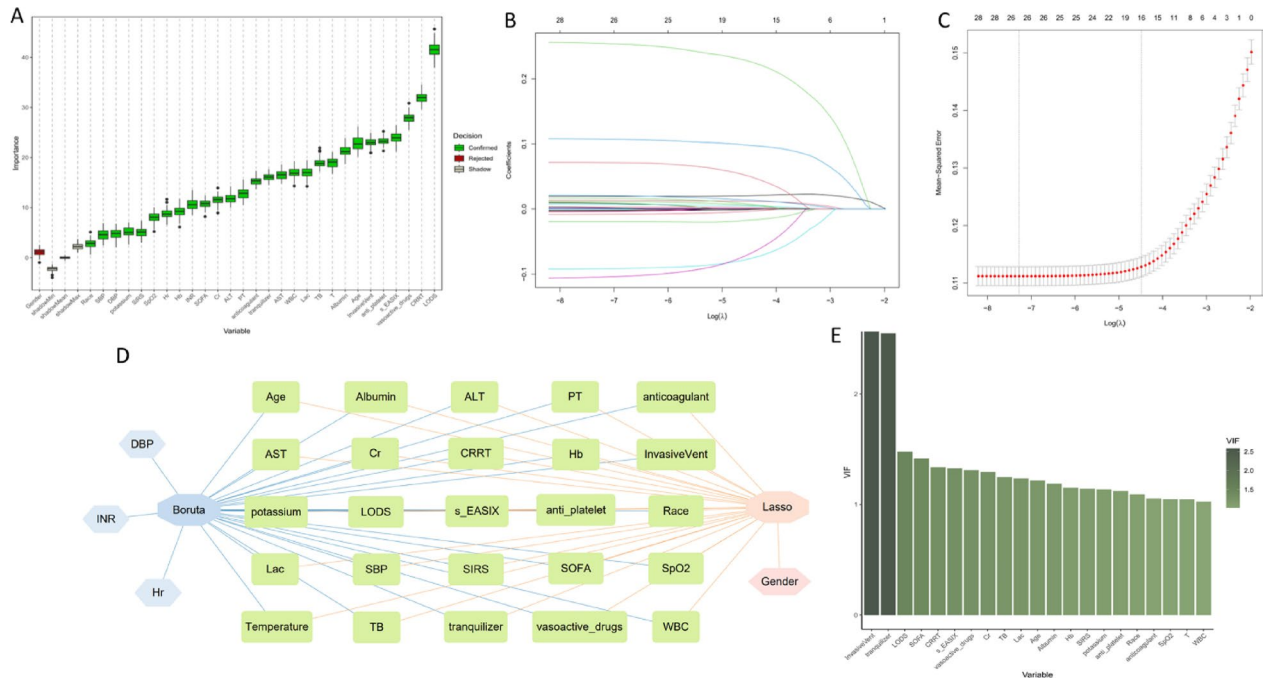


Fig. 5. Feature variable selection for 30-d all-cause mortality in the ICU. **(A)** Feature selection by the Boruta algorithm. Vertical axis: Z-scores of variables, with green indicating acceptable variables. **(B, C)** Coefficient paths of LASSO regression and cross-validation error curves. **(D)** Venn diagram for feature selection. **(E)** Multicollinearity test by VIF.

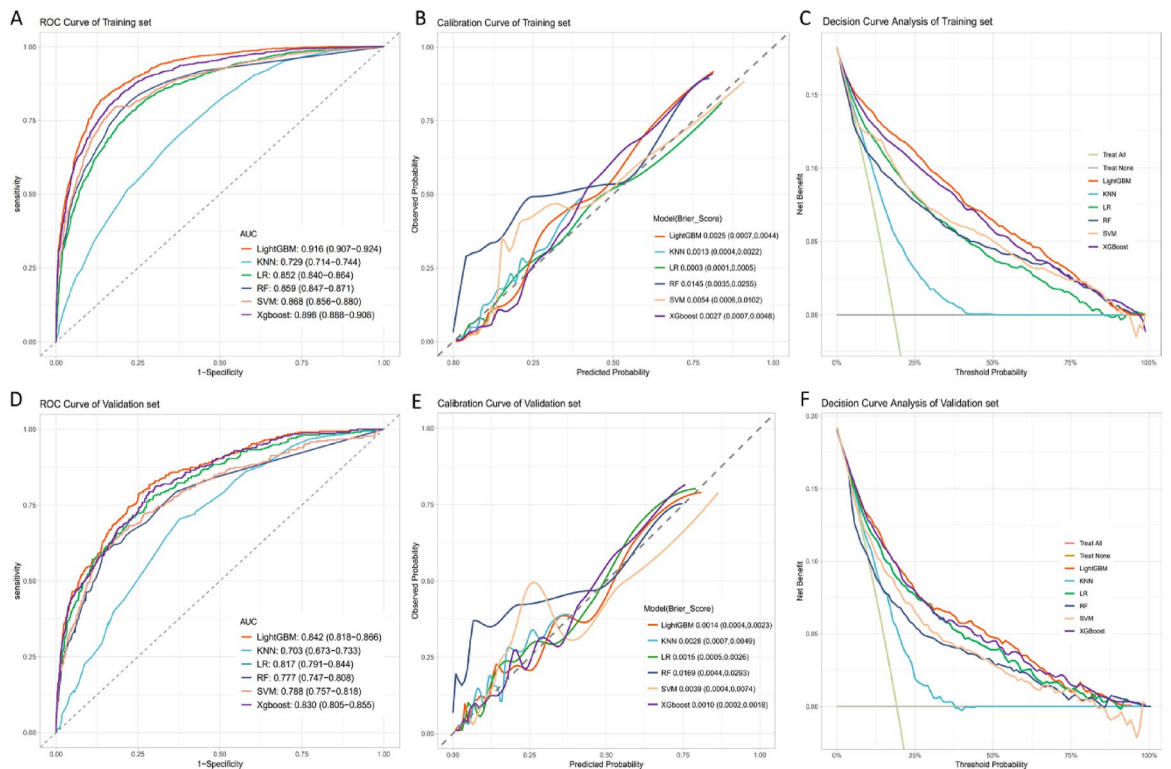


Fig. 6. Comprehensive assessment of model performance in the training set **(A–C)** and validation set **(D–F)**. **(A, D)** ROC curves. **(B, E)** Calibration curves. **(C, F)** Decision curves.

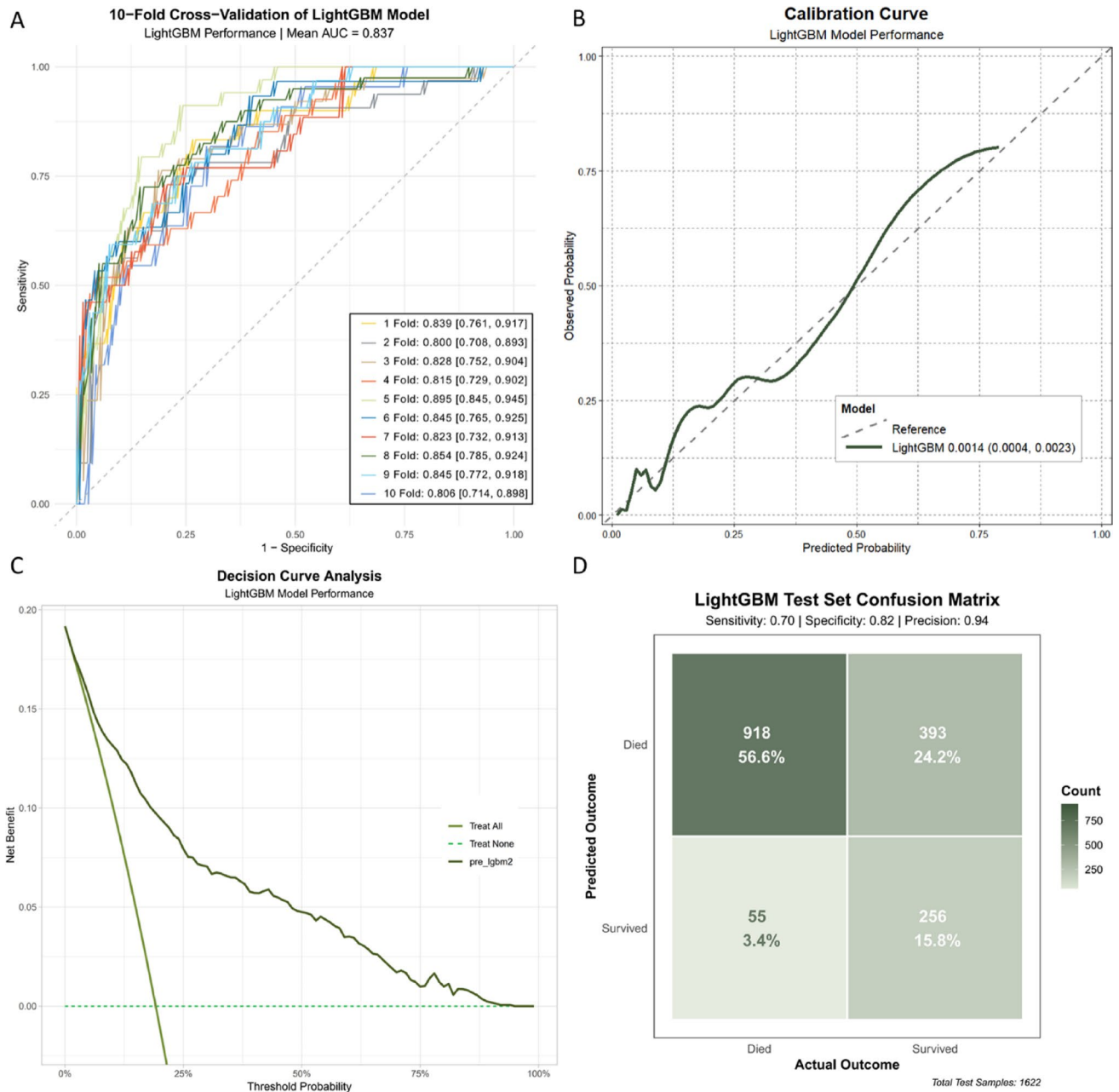


Fig. 7. Comprehensive performance assessment of the optimal model (LightGBM). (A) tenfold cross-validation curves; (B) Calibration curves; (C) Decision curves; (D) Confusion matrix (tenfold cross-validation).

of vascular reactivity and multiple organ dysfunction syndrome^{8,10}. In the acute phase of sepsis, the intense inflammatory response triggers metabolic reprogramming. To meet the surging demands of immune cells for energy, the cellular metabolism shifts from oxidative phosphorylation to aerobic glycolysis²⁹. During this process, immune cells are activated and glycolysis is enhanced, which improves the expression and activity of LDH, a key glycolytic enzyme, to meet energy demands in acute inflammation. This metabolic shift is accompanied by and exacerbates endothelial cell injury, resulting in massive LDH release into the bloodstream^{22,30}. Therefore, persistently elevated or chronically high serum LDH serves as a marker of uncontrolled inflammatory response and persistent endothelial injury. Additionally, large amounts of inflammatory cytokines (e.g., TNF- α , IL-1 β , and IL-6) are released by immune cells upon activation by bacteria. Then they bind to Toll-like receptor 4 on the platelet surface to initiate platelet activation via downstream MyD88-dependent pathways^{31,32}. Once platelets are activated, the inflammatory response will be further amplified, and platelet aggregation is enhanced, creating a positive feedback loop of “activation-release-reactivation”³³. Platelets, immune cells, and vascular endothelium that interact with each other form microthrombi at infection sites as a defense against pathogen spread. However, “immunothrombosis” often becomes overactivated due to uncontrolled infections. This leads to more platelet

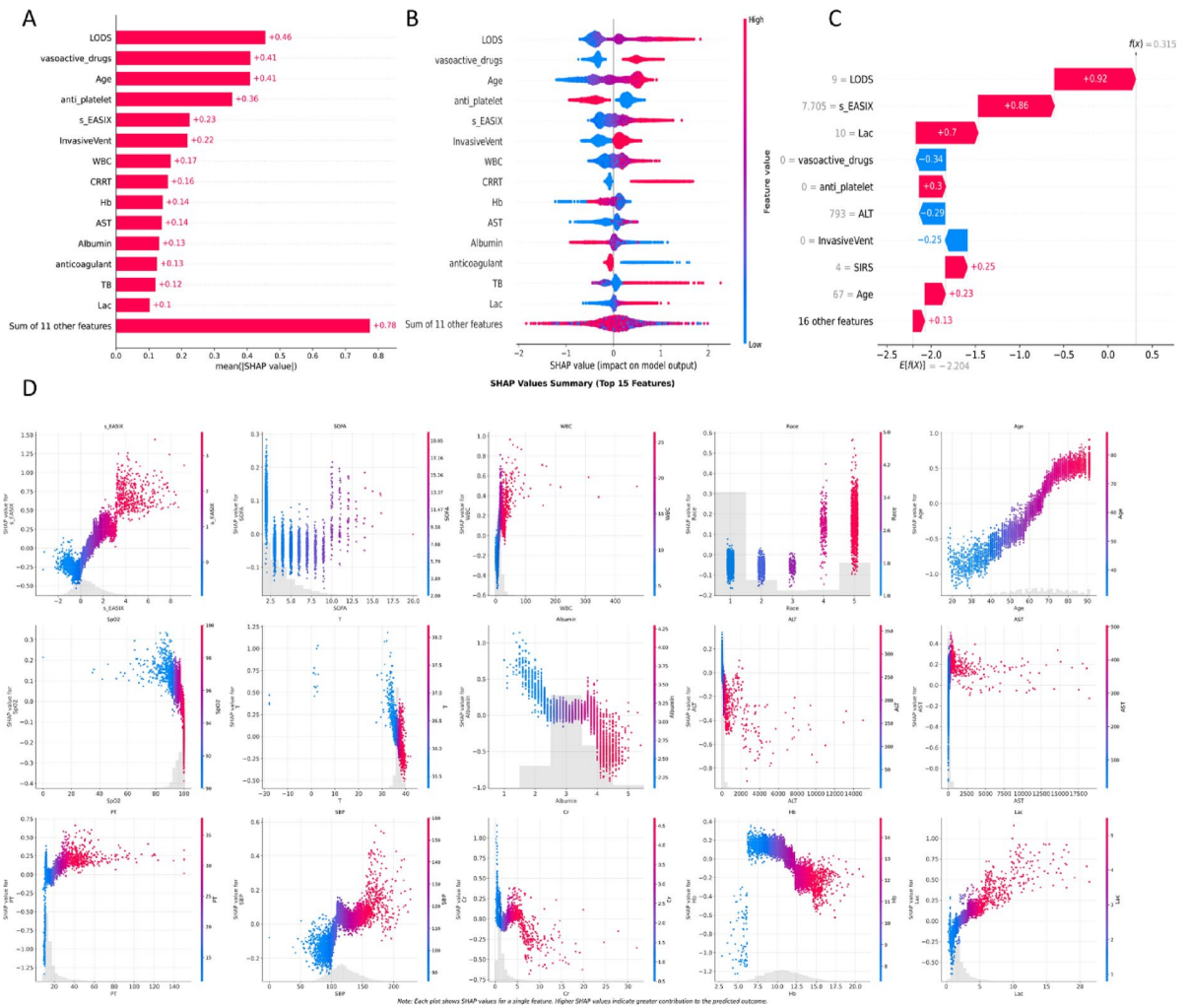


Fig. 8. Global model interpretation by SHAP values. **(A)** SHAP bar chart. Core predictors and their contributions are marked in descending order of mean absolute SHAP values. **(B)** SHAP dot plot. The horizontal position of dots indicates the SHAP values of samples, while color coding indicates feature values. **(C)** SHAP waterfall plot. Cumulative contributions of features to output. **(D)** SHAP dependence plot. The principal curve characterizes the function relation between feature values and SHAP values, while the scatter distribution shows the sample density.

consumption beyond the production of bone marrow megakaryocytes, and causes a sharp decline in platelet counts, microcirculatory impairment, and organ damage^{34–36}. These studies suggest that integrating LDH and platelet counts may possess superior value in prognostic evaluation. Therefore, considering the crucial role of endothelial dysfunction in sepsis pathophysiology, we selected s-EASIX, a marker for endothelial dysfunction, as the entry point to explore its relation with sepsis prognosis.

Western Blot and qPCR are the detection methods for traditional endothelial injury markers (e.g., vWF, sICAM-1), which are complex and expensive^{37–39}. As novel biomarkers for assessing vascular endothelial injury, the EASIX/s-EASIX can be calculated using routine biochemical indicators. It displays important clinical value in the prognostic management of cerebral infarction, coronary heart disease, and diabetes^{15,40}. However, the EASIX incorporates creatinine, potentially overestimating the severity of endothelial injury in patients with renal impairment. This bias of EASIX can be avoided by s-EASIX which focuses specifically on endothelial function assessment of non-renal origin and possesses similar dynamic trends to EASIX^{16,17}. In sepsis, elevated EASIX is parallel with VEGF concentration, both of which have predictive value for early mortality odds⁴¹. Therefore, in clinical settings dominated by non-renal diseases, s-EASIX may achieve a more specific assessment of endothelial function.

Longitudinal data provide more information about disease progression than the s-EASIX at specific time points⁴². Trajectory analysis can identify change trends in repeated measurement indicators. In this study, patients with a medium (at ICU admission) but continuously rising s-EASIX trajectory experienced significantly worse outcomes. The prognosis was comparable between patients with an initially high but rapidly falling trajectory and those with a continuously low trajectory. It can be inferred that sustained elevation of s-EASIX may reflect persistent endothelial dysfunction, accompanied by aggravation of vascular dysregulation and microcirculatory

dysfunction, thus jointly raising the risk of MODS and adverse outcomes^{10,22}. Furthermore, subgroup analyses revealed a significant interaction between age and indicators, with younger patients exhibiting higher mortality odds than older ones. The possible reason is that the strong immune systems of younger patients are more prone to triggering intense inflammatory responses when exposed to severe stressors, causing more severe endothelial injury. Since younger patients have good baseline conditions, high s-EASIX is a strong signal of compensatory capacity breakdown. In contrast, the incremental risk indicated by elevated s-EASIX may be diluted or confounded by immunosenescence, baseline endothelial dysfunction, comorbidities, and competing mortality odds in elderly patients^{43,44}. In addition, the available ML model based on traditional indicators has a C-index of only 0.774 in the validation set⁴⁵, whereas the model effectively integrating dynamic biomarkers in this study displayed superior discrimination power (AUC 0.842). Notably, emerging indicators such as the stress hyperglycemia ratio and leukocyte trajectories have been incorporated into modeling in some studies. However, they are not important roles in the final model prediction according to the SHAP analysis^{46,47}.

This study has the following main innovations. First, we systematically focused on the dynamic trajectories of s-EASIX and deeply analyzed its prognostic value in ICU sepsis patients. More importantly, this study not only verified the predictive power of s-EASIX from a longitudinal evolution perspective but also addressed the model's "black-box effect" by SHAP interpretability analysis. The findings revealed the contribution of s-EASIX as a key feature, enhancing model transparency and clinical credibility.

Therefore, the s-EASIX can be transformed into an interpretable clinical decision-making tool, enabling earlier and more personalized dynamic stratification of mortality odds and creating windows of opportunity for intervention. Some limitations are worth noting. First, potential data biases may be introduced in this single-center retrospective study based on MIMIC-IV. Second, due to multiple complex factors involved, the underlying pathophysiological mechanism by which the s-EASIX trajectory changes lead to elevated mortality could not be inferred. Third, despite the powerful internal performance of the ML model, external validation across cohorts is required before clinical use. Finally, further cohort studies are warranted to enhance predictive accuracy. Furthermore, we believe the clinical value of the s-EASIX dynamic trajectory should be expanded to therapeutic decision support beyond prognostic prediction. A sustained upward trend of the s-EASIX trajectory can serve as a critical early warning signal for vascular coagulation disorders and organ function deterioration, creating a crucial opportunity for early intervention. Meanwhile, this trajectory holds promise for quantitatively assessing endothelial injury and thrombotic risks associated with vasoactive agents and anticoagulant therapy, thereby advancing personalized and dynamic development of treatment management.

Conclusion

This study identified five distinct classes of s-EASIX dynamic trajectories in sepsis patients using a GMM. They exhibited great heterogeneity in clinical outcomes and organ support requirements and were considered independent prognostic factors for sepsis. The s-EASIX dynamic trajectory demonstrated higher discriminative accuracy in clinical outcomes than a single static measurement. To further assess the predictive value of s-EASIX in prognosis, it was incorporated into baseline data, and a LightGBM was created. The verification results confirmed the good predictive performance of this prediction model. The s-EASIX was identified by SHAP interpretability analysis as a key feature in this model.

Data availability

The raw data are available from the corresponding author upon reasonable request. The data presented in this study are openly available in the MIMIC-IV (v3.1) (<https://physionet.org/content/mimiciv/3.1/>).

Received: 19 September 2025; Accepted: 12 February 2026

Published online: 26 February 2026

References

1. Evans, L. et al. Surviving sepsis campaign: International guidelines for management of sepsis and septic shock 2021. *Crit Care Med.* **49**(11), e1063–e1143 (2021).
2. Novosad, S. A. et al. Vital signs: Epidemiology of sepsis—Prevalence of health care factors and opportunities for prevention. *MMWR Morb. Mortal. Wkly. Rep.* **65**(33), 864–869 (2016).
3. Xu, J. Q. et al. Viral sepsis: Diagnosis, clinical features, pathogenesis, and clinical considerations. *Mil. Med. Res.* **11**(1), 78 (2024).
4. Küster, H. et al. Interleukin-1 receptor antagonist and interleukin-6 for early diagnosis of neonatal sepsis 2 days before clinical manifestation. *Lancet* **352**(9136), 1271–1277 (1998).
5. He, R. R. et al. Sepsis biomarkers: Advancements and clinical applications—a narrative review. *Int. J. Mol. Sci.* <https://doi.org/10.3390/ijms25169010> (2024).
6. Hernandez, G., Bellomo, R. & Bakker, J. The ten pitfalls of lactate clearance in sepsis. *Intensive Care Med.* **45**(1), 82–85 (2019).
7. Gong, F. et al. H3K14la drives endothelial dysfunction in sepsis-induced ARDS by promoting SLC40A1/transferrin-mediated ferroptosis. *MedComm* **6**(2), e70049 (2025).
8. Joffre, J. et al. Endothelial responses in sepsis. *Am J Respir Crit Care Med.* **202**(3), 361–370 (2020).
9. Li, W. et al. Classic signaling pathways in alveolar injury and repair involved in sepsis-induced ALI/ARDS: New research progress and prospect. *Dis. Markers* **2022**, 6362344 (2022).
10. Tang, F. et al. Endothelial dysfunction: Pathophysiology and therapeutic targets for sepsis-induced multiple organ dysfunction syndrome. *Biomed. Pharmacother.* **178**, 117180 (2024).
11. Wu, M. et al. Effect of endothelial responses on sepsis-associated organ dysfunction. *Chin. Med. J.* **137**(23), 2782–2792 (2024).
12. Korell, F. et al. Pre-transplant EASIX and sepsis after allogeneic stem cell transplantation. *Intensive Care Med.* **48**(6), 753–755 (2022).
13. Xu, H. B. et al. Association between endothelial activation and stress index and 28-day mortality in septic ICU patients: A retrospective cohort study. *Int. J. Med. Sci.* **20**(9), 1165–1173 (2023).
14. Estler, B. et al. Endothelial dysfunction assessed by the endothelial activation and stress index (EASIX) predicts risk of mortality in chronic heart failure patients. *Int. J. Cardiol.* **438**, 133566 (2025).

15. Sang, M. et al. Association between endothelial activation and stress index and 30-day mortality risk in acute myocardial infarction patients: A study based on the medical information mart for intensive care-IV database. *BMC Cardiovasc. Disord.* **24**(1), 699 (2024).
16. Gavriilaki, E. et al. Soluble urokinase-type plasminogen activator receptor (suPAR), growth differentiation factor-15 (GDF-15), and soluble C5b-9 (sC5b-9) levels are significantly associated with endothelial injury indices in CAR-T cell recipients. *Int. J. Mol. Sci.* <https://doi.org/10.3390/ijms252011028> (2024).
17. de Boer, J. W. et al. Population-based external validation of the EASIX scores to predict CAR T-cell-related toxicities. *Cancers* <https://doi.org/10.3390/cancers15225443> (2023).
18. Johnson, A. E. W. et al. MIMIC-IV, a freely accessible electronic health record dataset. *Sci. Data* **10**(1), 1 (2023).
19. Singer, M. et al. The third international consensus definitions for sepsis and septic shock (Sepsis-3). *JAMA* **315**(8), 801–810 (2016).
20. Pedraza, A. et al. Easix score correlates with endothelial dysfunction biomarkers and predicts risk of acute graft-versus-host disease after allogeneic transplantation. *Transplant Cell Ther.* **30**(2), 187.e181–187.e112 (2024).
21. Peña, M. et al. Pretransplantation EASIX predicts intensive care unit admission in allogeneic hematopoietic cell transplantation. *Blood Adv.* **5**(17), 3418–3426 (2021).
22. Yu, H. et al. A positive correlation between serum lactate dehydrogenase level and in-hospital mortality in ICU sepsis patients: evidence from two large databases. *Eur. J. Med. Res.* **29**(1), 525 (2024).
23. Wang, J., Fei, W. & Song, Q. One-year mortality prediction for patients with sepsis: A nomogram integrating lactic dehydrogenase and clinical characteristics. *BMC Infect. Dis.* **23**(1), 668 (2023).
24. Zhou, Z. et al. Clinical predictive value of short-term dynamic changes in platelet counts for prognosis of sepsis patients in intensive care unit: a retrospective cohort study in adults. *Zhonghua Wei Zhong Bing Ji Jiu Yi Xue* **32**(3), 301–306 (2020).
25. Ye, Q. et al. Serial platelet count as a dynamic prediction marker of hospital mortality among septic patients. *Burns Trauma* **12**, tkae016 (2024).
26. Claps, G. et al. The multiple roles of LDH in cancer. *Nat. Rev. Clin. Oncol.* **19**(12), 749–762 (2022).
27. Li, S. et al. The dynamic role of platelets in cancer progression and their therapeutic implications. *Nat. Rev. Cancer* **24**(1), 72–87 (2024).
28. Liu, J. et al. The values of PDK1 and LDH levels in patients with sepsis and septic shock: A prospective observational study. *J. Inflamm. Res.* **17**, 6815–6826 (2024).
29. Fu, X. Z. & Wang, Y. Interferon- γ regulates immunosuppression in septic mice by promoting the Warburg effect through the PI3K/AKT/mTOR pathway. *Mol. Med.* **29**(1), 95 (2023).
30. Pan, T. et al. Immune effects of PI3K/Akt/HIF-1 α -regulated glycolysis in polymorphonuclear neutrophils during sepsis. *Crit. Care.* **26**(1), 29 (2022).
31. Lumadue, J. A. et al. Cytokine induction of platelet activation. *Am. J. Clin. Pathol.* **106**(6), 795–798 (1996).
32. Iba, T. & Levy, J. H. Inflammation and thrombosis: Roles of neutrophils, platelets and endothelial cells and their interactions in thrombus formation during sepsis. *J. Thromb. Haemost.* **16**(2), 231–241 (2018).
33. Maneta, E. et al. Endothelial dysfunction and immunothrombosis in sepsis. *Front. Immunol.* **14**, 1144229 (2023).
34. Martinod, K. & Deppermann, C. Immunothrombosis and thromboinflammation in host defense and disease. *Platelets* **32**(3), 314–324 (2021).
35. Giustozzi, M. et al. Coagulopathy and sepsis: Pathophysiology, clinical manifestations and treatment. *Blood Rev.* **50**, 100864 (2021).
36. Iba, T., Levi, M. & Levy, J. H. Sepsis-induced coagulopathy and disseminated intravascular coagulation. *Semin. Thromb. Hemost.* **46**(1), 89–95 (2020).
37. Huang, Y. et al. Endothelial activation and stress index is a reliable predictor for the prevalence and mortality outcomes of stroke. *Sci. Rep.* **15**(1), 23285 (2025).
38. Li, J. C. et al. A study of relation between changes in serum soluble intercellular adhesion molecule and infarction volume in patients with acute cerebral infarction. *Zhongguo Wei Zhong Bing Ji Jiu Yi Xue* **20**(11), 660–662 (2008).
39. Small, A. M. et al. Lipoprotein(a), C-reactive protein, and cardiovascular risk in primary and secondary prevention populations. *JAMA Cardiol.* **9**(4), 385–391 (2024).
40. Xier, Z. et al. Plasma VWF: Ag levels predict long-term clinical outcomes in patients with acute myocardial infarction. *Front. Cardiovasc. Med.* **9**, 1013815 (2022).
41. Tang, A. L. et al. Prognostic role of elevated VEGF in sepsis: A systematic review and meta-analysis. *Front. Physiol.* **13**, 941257 (2022).
42. Zhao, L. et al. Incorporating longitudinal biomarkers for dynamic risk prediction in the era of big data: A pseudo-observation approach. *Stat. Med.* **39**(26), 3685–3699 (2020).
43. Li, X. et al. Inflammation and aging: signaling pathways and intervention therapies. *Signal Transduct. Target Ther.* **8**(1), 239 (2023).
44. Franceschi, C. et al. Inflamm-aging. An evolutionary perspective on immunosenescence. *Ann. N. Y. Acad. Sci.* **908**, 244–254 (2000).
45. Zhang, Y. et al. Machine learning for the prediction of sepsis-related death: A systematic review and meta-analysis. *BMC Med. Inform. Decis. Mak.* **23**(1), 283 (2023).
46. Yan, F. et al. Association between the stress hyperglycemia ratio and 28-day all-cause mortality in critically ill patients with sepsis: A retrospective cohort study and predictive model establishment based on machine learning. *Cardiovasc. Diabetol.* **23**(1), 163 (2024).
47. Miao, S. et al. Clinical subtypes identification and feature recognition of sepsis leukocyte trajectories based on machine learning. *Sci. Rep.* **15**(1), 12291 (2025).

Acknowledgements

Not applicable.

Author contributions

Kong Zhenghui: Conceptualization, Methodology, Data curation, Software; Liu Yuwei: Conceptualization, Data curation, Software, Validation, Writing—Original draft preparation; Zeng Zhiyi: Data curation, Software; Liu Zhiyu: Data interpretation; Kong Zhenghui: Validation, Writing—Original draft preparation; Chen Huilong and Guo Hong: Data curation, Visualization, Investigation; Liu Qiujiang: Methodology, Writing—Reviewing and Editing. All authors reviewed and approved the final manuscript submitted.

Funding

This research did not receive any specific grant from funding agencies in the public, commercial, or not-for-profit sectors.

Declarations

Competing interests

The authors declare no competing interests.

Ethical approval and consent to participate

Ethical review and approval were waived for this study, as it was conducted using publicly available from the MIMIC-IV (v3.1). Approval for the research use of these data was obtained from the BIDMC Institutional Review Board.

Additional information

Supplementary Information The online version contains supplementary material available at <https://doi.org/10.1038/s41598-026-40400-1>.

Correspondence and requests for materials should be addressed to Q.L.

Reprints and permissions information is available at www.nature.com/reprints.

Publisher's note Springer Nature remains neutral with regard to jurisdictional claims in published maps and institutional affiliations.

Open Access This article is licensed under a Creative Commons Attribution-NonCommercial-NoDerivatives 4.0 International License, which permits any non-commercial use, sharing, distribution and reproduction in any medium or format, as long as you give appropriate credit to the original author(s) and the source, provide a link to the Creative Commons licence, and indicate if you modified the licensed material. You do not have permission under this licence to share adapted material derived from this article or parts of it. The images or other third party material in this article are included in the article's Creative Commons licence, unless indicated otherwise in a credit line to the material. If material is not included in the article's Creative Commons licence and your intended use is not permitted by statutory regulation or exceeds the permitted use, you will need to obtain permission directly from the copyright holder. To view a copy of this licence, visit <http://creativecommons.org/licenses/by-nc-nd/4.0/>.

© The Author(s) 2026